Microfabrication of High Temperature Silicon Devices Using Wafer Bonding and Deep Reactive Ion Etching

Amit Mehra, Arturo A. Ayón, Ian A. Waitz, and Martin A. Schmidt

Portions of this work were presented at the Transducers Research Foundation Hilton Head Workshop on Solid-State Sensors and Actuators, 1998. Amit Mehra and Ian A. Waitz are with the Gas Turbine Laboratory, Department of Aeronautics and Astronautics, Massachusetts Institute of Technology, Cambridge, MA 02139. Arturo A. Ayón and Martin A. Schmidt are with the Microsystems Technology Laboratories, Department of Electrical Engineering and Computer Science, Massachusetts Institute of Technology, Cambridge, MA 02139.

Abstract

As part of an effort to develop a micro gas turbine engine capable of providing 10-50 Watts of electrical power in a package less than one cubic centimeter in volume, we report the fabrication and testing of the first hydrogen combustor micromachined from silicon. Measuring 0.066 cm^3 in volume, and complete with a fuel manifold and set of fuel injector holes, the fabrication of the device was largely enabled by the use of Deep Reactive Ion Etching (DRIE) and **aligned** silicon wafer bonding. The 150 Watt microcombustor has a power density in excess of 2000 MW/m^3 and has been successfully demonstrated to provide turbine inlet temperatures up to 1800K. After fifteen hours of experimental tests, the combustor maintained its mechanical integrity and did not exhibit any visible damage. Combined with the results of a materials oxidation study, these tests are used to demonstrate the satisfactory performance of silicon in the harsh oxidizing environment of a combustion chamber.

I. Introduction

Micro heat engines employing gas turbine components have recently been introduced as a potential means for generating power [1]. The increased power density resulting from the cube-square law[1], combined with the higher strength-to-density ratio of silicon micro-structures makes such devices an attractive prospect [2]. The realization of power-MEMS however, poses new fabrication challenges. While preliminary results do indeed suggest their manufacturability [3], the requirement for complex fluid channels and high aspect ratio structures is complicated by the high temperature operating environment of the engine. The presence of a combustion chamber to convert the chemical energy of a fuel into fluid thermal and kinetic energy necessitates gas temperatures close to the melting point of silicon [4]. Thus, the ability of silicon structures to withstand these working conditions needs to be investigated.

As part of the MIT microengine project introduced and motivated by Epstein *et al.* [5], an effort is currently underway to develop a micro gas turbine engine capable of producing 10-50W of electrical power in a package less than one cubic centimeter in volume. This paper concentrates on the fabrication aspects of a hydrogen combustor for this engine.

[1]Since the power output of an engine scales with mass flow, and hence the area, and the weight scales with the volume, the power density of a microengine linearly increases as the size of the device is reduced. The linear increase in power density however, is hindered by the additional **thermal and** fluid losses that are incurred at the micro-scale.

The primary contribution of this work is the microfabrication and testing of a device that is capable of running at gas temperatures several hundred degrees above the melting point of silicon, while providing power densities higher than those achieved by large-scale combustors used for power generation or aircraft engine applications.

We first begin with a brief review of silicon power-MEMS previously reported in the literature. The fabrication and testing of the hydrogen microcombustor is presented next. Section III describes the microfabrication process; test data is presented in Section IV. The results of a materials study that establish the viability of using silicon in such devices are also reported in Section IV. Finally, Section V includes a summary and conclusions.

II. Silicon Power-MEMS

The microengine is mainly targeted for portable power generation and micro air vehicle propulsion. For these applications, the power density of the energy conversion unit is the primary figure of merit. Therefore, before presenting the results for the microfabricated silicon combustor, we briefly review chemical, electrical, magnetic and solar power-MEMS previously reported in the literature. This section is primarily intended to summarize the power density levels that have been achieved to date using silicon microfabricated devices.

Silicon microfabrication concepts have been identified as a viable means of miniaturizing chemical reactors to improve chemical process development and operation [6]-[8]. Although these reactors are not intended for power generation, the exothermic partial oxidation reactions employed in these processes can generate substantial thermal energy. Microfabricated chemical reactors have been reported by Jensen *et al.* [9] and Srinivasan *et al.* [10], [11]. The T-shaped reactor features a 18 mm $\times$ 1.3 mm $\times$ 0.55 mm reaction zone that can be used to study the catalytic partial oxidation of ammonia. Typical experiments produced approximately 0.25 Watts of power from the heat of reaction, resulting in power densities of the order of 20 MW/m^3.

Since motors use electrical or magnetic power to generate mechanical torque, they can also be categorized as silicon power-MEMS. Electric motors are reported to have generated 100 μWatts, the power density being approximately 1.7 MW/m^3 (Tai [12], Mehregany [13], [14]). Magnetic micromotors fabricated by Ahn and Allen [15], [16] have a power output of 60 μWatts and a power density of 200 MW/m^3. It should be noted that these

numbers are based on the field density of the air gap only; since the dimensions of the device are much larger, the *device* power density per unit volume will be lower.

Miniaturized solar cells and lithium microbatteries have also been proposed as integrated power sources for MEMS applications. Solar cell arrays generate approximately 400 μWatts; the estimated power density being $\sim$1 MW/m^3 [17]. Rechargeable solid state lithium microbatteries are reported to produce 40 μWatts at a power density of 0.4 MW/m^3 [18].

In addition to microfabricated silicon power-MEMS, conventionally fabricated devices have also been used to generate power at similar scales. In particular, metallic channel flow reactors employing controlled H_2-O_2 reactions have been used as heat exchangers and evaporators [19]-[21]. Using a platinum catalyzed reaction of H_2 and O_2, Hagendorf *et al.* [21] have reported a maximum heat generation of 150 Watts in 1 cm^3 volume. This corresponds to a power density of 150 MW/m^3.

The power density of the devices mentioned above are summarized in Table I. While this is not an exhaustive review of all the silicon power-MEMS reported in the literature, it tabulates the power levels that have been achieved to date, and serves to place this research in the perspective of what has been done before.

We now present the fabrication and test results for the silicon microcombustor

III. Fabrication of the Microcombustor

The microcombustor assembly consists of three fusion-bonded silicon wafers. A scanning electron micrograph of the final microfabricated silicon combustor is shown in Figure 1, along with a schematic illustration of the fuel and air flow paths, the fuel manifold and injector holes, and the combustor inlet ports. Air enters the device axially from the top, makes a right angle turn and flows radially outward through a duct where the compressor would be housed. Hydrogen is injected downstream of the compressor **region** through fuel injector holes and is allowed to mix with the air before entering the combustion chamber through the axial inlet ports. The mixture burns in an annular-shaped chamber and finally exits axially through a circular exhaust. In an engine application, the flow would pass through a turbine for power extraction prior to being exhausted.

The overall combustor arrangement was set by preliminary design studies for the micro

Device	**Power density (MW/m^3)**
Micro-lithium batteries [18]	0.4
Micro solar cells [17]	1
Micro-electric motors [14]	1.7
Microreactors (silicon) [11]	20
Large-scale combustors [4]	40
Micro channel reactors (metal) [21]	150
Micro-magnetic motors [16]	200
Silicon microcombustor	2000

TABLE I

A COMPARISON OF THE POWER DENSITY LEVELS ACHIEVED BY VARIOUS DEVICES.

gas turbine engine [5], [22]. The axial length and volume of the combustor were chosen in accordance with computational fluid dynamics (CFD) predictions for the minimum volume necessary for complete combustion at atmospheric pressure. The combustion chamber is an annular region 1 mm in height, with volume of 66 mm^3, and an inner and outer diameter of 5 mm and 10 mm respectively.

The fuel injector size and spacing was based on semi-empirical models for normal jet injection and mixing to satisfy lateral spreading and penetration requirements [4]. The final device consisted of a total of 76 injector holes with a diameter of 30 μm, equally spaced at a radius of 3 mm. A total of 24, 340 μm diameter combustor inlet ports were designed to eliminate upstream propagation of the flame into the compressor exit flow path.

The fabrication of the device required a total of six masks, including one that contained wafer-level alignment marks. A combination of four **dry** isotropic and two **dry** anisotropic etches were used to define the various components.

The fabrication process is illustrated via schematics of the wafer cross-sections in Fig-

ure 2. First, the top side of each of the wafers was coated with photoresist and patterned with the appropriate fuel manifold, spacer plate and combustion chamber geometry. The 200 μm deep fuel manifold and spacer plate, and half of the 1000 μm deep combustion chamber were isotropically **dry** etched. Since none of these features required parallel side walls, isotropic etching was chosen to minimize process time[2]. After completing the top side etches, the bottom side of the wafers were coated with resist; infra-red alignment was used to pattern the corresponding fuel injectors, combustor inlet ports and combustion chamber geometry on the bottom side. The 200 μm deep fuel injectors and combustor inlet ports were then anisotropically **dry** etched. (The combustion chamber was etched from both sides to limit the run-out in the side walls of the combustor).

Following the completion of individual processing, the three wafers were align-bonded. The 1.8 mm thick wafer stack was finally die-sawed to obtain thirteen 1.5 cm $\times$ 1.5 cm dies from the 100 mm wafer. Individual scanning electron micrographs of each of the wafers is shown in Figures 3 through 5. The major fabrication steps are explained as follows:

A. Photolithography

For all of the deep etches, the wafer surfaces were patterned using techniques similar to those reported in [23]. Following a dehydration bake in an HMDS (hexamethyldisilazane) oven, approximately 10 μm of thick positive photoresist (Hoechst, AZ-4620) was spun cast on the wafer surface. The resist was pre-baked for one half hour in a 90°C convection oven and then exposed using a contact mask aligner with a UV light source. After developing in AZ 440 MIF, the photolithography was completed with a post-bake in a 120°C ambient.

B. Deep Reactive Ion Etching

Following the evolution of Bosch's patented technique for time-multiplexed deep etching (TMDE) [24], DRIE combined with silicon fusion bonding are becoming enabling technologies for MEMS devices [25], [26]. Likewise, the use of DRIE to etch high aspect ratio structures for complex fluid paths is also critical for the fabrication of the microcombustor test rig.

[2]Compared to etch rates of approximately 3 μm/min for anisotropic etching, rates of up to 7 μm/min could be achieved using isotropic etches.

The microcombustor was fabricated using a combination of dry isotropic and anisotropic etches. The isotropic etches employed straight SF_6 chemistry. The anisotropic etches used a time-multiplexed inductively coupled plasma of SF_6 as the etchant and C_4F_8 as the side wall passivating polymer. The performance of the etcher was optimized by characterizing the etches over a wide parameter space [27], allowing fabrication of high tolerance and high aspect ratio structures such as the 30 μm diameter, 200 μm deep fuel injector holes.

In all through-etches, photoresist was used to attach quartz handling wafers to the bottom of the wafer. This maintained the vacuum seal for the helium cooling on the back side as the etch penetrated through the wafer.

C. Aligned Wafer Bonding

After individual processing, each of the wafers were put through a standard RCA clean [28]. They were then align-bonded using a commercial aligner **(Electronic Visions, Inc.)**. The bonding was completed in two steps - the first and second wafers were bonded first; the stack was then annealed, RCA cleaned, and finally bonded to the third wafer. Consistent with results reported in [29], a one hour post-bond anneal in an inert ambient at 1100°C was found to significantly improve bond quality. Figure 6 shows an infra-red image of the double-bonded three-wafer stack. Although the image shows large fringes indicating poor quality of the bond along the edges of the wafer, over 80% of the die survived the die-saw process. Out of a possible sixteen, thirteen fully-bonded and complete microdevices were finally obtained. It should be noted that these results represent one of the earlier attempts at multiple wafer bonds. **Since then, the wafer bonding protocol has been changed. The wafers are now bonded in a vacuum and the tooling has been modified such that it contacts the wafer at only three point locations. These changes have recently resulted in nearly 100% yields at die-saw for devices with similar multiple wafer bonds [3].**

Following the completion of the fabrication process, the microcombustors were tested by clamping the structure in a set of invar plates. A 3-D exploded schematic of the assembled rig is shown in Figure 7. The invar plates served a dual function - they provided macro fluidic connections for fuel and air and also housed thermocouple temperature diagnostics for measurement of combustor wall and exit gas temperatures. The atmospheric test

results for the hydrogen-fueled combustor are presented in the following section.

IV. Test Results

A. Atmospheric Pressure Combustion Tests

Atmospheric pressure test results were obtained for hydrogen-air combustion over most of the flammability range. While detailed results for combustion exit temperatures and efficiencies were reported in [30], only selected results for the wall and exit gas temperature are presented herein. Figure 8 plots the gas temperatures measured at the exit of the combustor as a function of the equivalence ratio[3]. This shows the satisfactory attainment of a combustor exit temperature in excess of 1600K that is necessary to complete the thermodynamic cycle and obtain useful power output from the micro gas turbine engine[4].

Even though desired turbine inlet temperatures were obtained, poor thermal isolation of the rig resulted in significant heat loss, thereby keeping the walls of the combustor relatively cooler than the gas temperatures. Figure 9 plots the temperature of the top and bottom invar plates that clamped the microfabricated device, and indicates that the combustor wall temperature remained well below the melting point of silicon[5].

Currently, efforts are underway to improve the thermal insulation of the rig and reduce the heat loss through the device to increase combustor efficiency. While improved thermal insulation is expected to increase the wall temperature, the reduction in fuel needed to achieve the desired turbine inlet temperatures would also correspondingly lower the combustion chamber temperature. This suggests that the walls could continue to operate at relatively cooler temperatures, even when thermal insulation and combustor efficiency are further increased.

[3]Equivalence ratio, which is a measure of the amount of fuel in the mixture, is the fuel-air ratio normalized by the **stoichiometric** value of the fuel-air ratio. **Thus, at an equivalence ratio of one, the fuel and air burn stoichiometrically with no excess oxygen or fuel.**

[4]Temperatures as high as 1800K were obtained for premixed hydrogen-air combustion. In this case, the fuel was mixed upstream of the fuel manifold instead of being injected through the injectors. The lower non-premixed temperatures are attributed to a misalignment of the wafers, resulting in a reduction of the mixing length on one side of the combustor, and hence, incomplete mixing.

[5]The results of a computational heat transfer analysis showed that the entire structure is isothermal within 100K. (This is expected given the high thermal conductivity of silicon, and hence, the low Biot numbers for the device). Consequently, in the absence of diagnostics to directly measure the silicon wall temperatures, the temperatures of the top and bottom invar walls were used as proxies.

Overall, while high pressure testing and improved combustor diagnostics still need to be employed, the combustor has been successfully tested to provide turbine inlet temperatures in excess of 1600K. With a fuel heating rate of approximately 150W (corresponding to a power density of 2000 MW/m^3), the device was tested for over fifteen hours. As shown in Figure 10, the combustor maintained its structural integrity and showed no visible damage. These results demonstrate the satisfactory performance of a micromachined silicon combustor for applications in a micro heat engine.

B. Materials, High Temperature Oxidation Results

As shown in Figure 10, post-combustion examination of the silicon microcombustor indicated oxidation patterns around the structure and the combustor inlet ports. A materials study was consequently undertaken to further quantify the effects of oxidation in a combustion environment.

As part of this study, a combustor plate consisting of "finger-like" structures with sizes between 20 μm $\times$ 500 μm $\times$ 450 μm and 1600 μm $\times$ 2000 μm $\times$ 450 μm was fabricated and tested inside the combustor. Shown in Figure 11, the plate was fabricated by anisotropically etching through a single 450 μm wafer.

The structure was exposed to a combustion environment for over eight hours at atmospheric pressures and flow temperatures in excess of 2000K[6]. Depending on the size and aspect ratio of the fingers, and hence the temperature at which they equilibrated, the fingers grew between 1 μm and 10 μm[7] of oxide. The oxide thickness is of the same order of magnitude as that predicted by the Deal-Grove passive oxidation model [31], suggesting that the "active-oxidation" of silicon is not an overriding concern for this particular application,

Although atmospheric testing failed to reveal any limiting failure mechanism, elevated pressure testing of the fingered combustor plate identified creep to be the failure mechanism for silicon in high temperature microcombustor environments. As shown in Figure 12, at

[6]While combustor exit temperatures were between 1600K and 1800K, the combustion *chamber* temperature was measured to be a few hundred degrees higher. The overall wall temperature was once again in the range of 1000K.

[7]**Most of the amorphous oxide was less than a couple of microns thick. Only the thinnest of the fingers grew 10 μm flakes of crystalline oxide. The cause of this crystalline growth and the subsequent cracking and stress-induced effects still need to be examined.**

fluid temperatures in excess of 2200K, several of the fingers were found to creep. The location of the point where the different fingers began to bend correlated well with a two-dimensional heat transfer model for the temperature distributions along the length of the fingers. This suggests that under these conditions, the creep failure of the fingers followed the brittle-to-plastic transition of silicon which occurs at approximately 900K.

Finally, as the last part of the oxidation study, tests were conducted to identify the effects of the high Mach number, high pressure and heat transfer environment of a turbine. Although atmospheric tests on static components showed that oxidation would not be a limiting factor in the operation of a silicon microcombustor, the effects in the turbine environment of a microengine are unknown. While the effects on the rotor cannot be assessed in the absence of a spinning structure[8], a set of 150 μm high turbine vanes (static nozzle guide vanes - NGV's), was exposed to the combustor exhaust to examine the effects of oxidation in a potentially erosive, high temperature and pressure, supersonic flow environment. A micrograph of several of the vanes is shown in Figure 13. The placement of the vane pack in the rig is illustrated in Figure 14.

Figure 15 shows before and after pictures of a turbine stator vane following a five hour exposure to combustion exhaust at 1800K and 2.5 atm., and at a mass flow of 0.1g/sec. While "pitting" and erosion is visible on the blade surface, the vanes maintain their overall structural integrity, there being no more than a 2% change in throat area, and hence mass flow. This establishes the survivability of a static vane structure in a high pressure, temperature and high Mach number flow environment, and is suggestive of the ability to build a combustor and engine static structure out of silicon.

Currently, efforts are underway to integrate the combustor with the engine; first engine tests are expected in the year 2000.

V. Conclusions

As part of an effort to develop a micro gas turbine engine using silicon microfabrication technologies, we reported the fabrication and testing of a hydrogen combustor microma-

[8]Efforts are currently underway to integrate a rotating turbine with the hot combustor exhaust to study creep failure. To date, computational finite element modeling (FEM) and materials test data have been used to predict the rotor structural performance [32].

chined from silicon. While DRIE and silicon wafer bonding were the enabling manufacturing technologies, the design, fabrication and testing of the device required the effective integration of disciplines as diverse as silicon microfabrication, fluid dynamics, heat transfer and combustion. The microfabricated silicon combustor has a chamber measuring less than 0.07 cubic centimeters, and an integral fuel manifold and fuel injector holes. It has been successfully demonstrated to sustain stable hydrogen combustion, providing exit temperatures in excess of 1600K. While the performance of silicon was found to be creep limited at elevated pressures and temperatures in excess of 2200K, the combustor has been successfully tested for over fifteen hours, thereby demonstrating the satisfactory performance of silicon in such harsh environments. Combined with the results of an oxidation study which showed that the performance of a silicon microcombustor will not be oxidation limited, these results are an important step towards establishing the viability of building a new generation of power-MEMS using silicon microfabrication technology.

Acknowledgments

We would first like to recognize and thank Professor Alan H. Epstein for his conception of the MIT microengine project, and for being a constant source of encouragement and inspiration. We are also grateful to all other members of the microengine team for their support during various stages of this research, especially Professor Stephen D. Senturia, C. C. Lin, and Dr. Reza Ghodssi for their invaluable comments and suggestions. Finally, special thanks to Diana Park for help with the figures.

This work was largely supported by the Army Research Office through Grant DAAHO4-95-1-0093, Dr. Richard Paur, program manager. All devices were fabricated at the MIT Microsystems Technology Laboratories. The help of the technicians and staff is gratefully acknowledged.

References

[1] Epstein *et al.*, "Power MEMS and Microengines", presented at the IEEE Conference on Solid State Sensors and Actuators, 1997.

[2] Epstein, A. H., Senturia, S. D., "Macro Power from Micro Machinery", Science, Volume 276, p. 1211, May 23, 1997.

[3] Lin *et al.*, "Fabrication of a Micro Turbine/Bearing Rig", Late News Poster Session, Solid-State Sensor and Actuator Workshop at Hilton Head, 1998.

[4] Waitz, I. A., Gauba, G., Tzeng, Y-S., "Combustors for Micro-Gas Turbine Engines", ASME Journal of Fluids Engineering, Vol. 20, pp. 109-117, March 1998.

[5] Epstein *et al.*, "Micro-Heat Engines, Gas Turbines, and Rocket Engines", presented at the 28^{th} AIAA Fluid Dynamics Conference, 1997 (AIAA 97-1773).

[6] Benson, R. S., Ponton, J. W., "Process Miniaturisation - A Route to Total Environmental Acceptability", Trans IChemE 71 A, pp. 160-168, 1993.

[7] Lerou *et al.*, "Microfabricated Minichemical Systems: Technical Feasibility", Microsystem Technology for Chemical and Biological Microreactors, DECHEMA Monographs, 132, Frankfurt am Main, p. 51, 1996.

[8] Lerou, J. J., Ng, K. M., "Chemical Reaction Engineering: A multiscale approach to a multiobjective task", Chemical Engineering Science 51, pp. 1595-1614, 1996.

[9] Jensen *et al.*, "Reaction Engineering for Microreactor Systems", Microreaction Technology, Proceedings of the First International Conference on Microreaction Technology, 1997.

[10] Srinivasan *et al.*, "Chemical Performance and High Temperature Characterization of Micromachined Chemical Reactors", International Conference on Solid-State Sensors and Actuators, Digest of Technical Papers, Volume 1, 1 C3.01, 1997.

[11] Srinivasan *et al.*, "Micromachined Reactors for Catalytic Partial Oxidation Reactions", Reactors, Kinetics, and Catalysis, AIChE Journal, Vol. 43, No. 11, pp. 3059-3069, November 1997.

[12] Tai, Y. C., Fan, L. S., Muller, R. S., "IC-processed micro-motors: design, technology and testing", Proc. Micro Electro Mechanical Systems, IEEE Robotics and Automation Council, pp. 1-6, 1989.

[13] Mehregany *et al.*, "Operation of Microfabricated Harmonic and Ordinary Side-Drive Motors", Proceedings: IEEE Workshop on Micro Electro Mechanical Systems, pp. 1-8, 1990.

[14] Mehregany M., "Microfabricated Silicon Electric Mechanisms", Ph.D. Thesis, Massachusetts Institute of Technology, Cambridge, MA, 1990.

[15] Ahn, C. H., Allen, M. G., "A Fully Integrated Micromagnetic Actuator with a Multilevel Magnetic Core", Digest, IEEE Solid State Sensor and Actuator Workshop, pp. 14-18, Hilton Head, 1992.

[16] Ahn, C. H., Kim, Y. J., Allen, M. G., "A Planar Variable Reluctance Magnetic Micromotor With Fully Integrated Stator and Wrapped Coils", Proc. Micro Electro Mechanical Systems, IEEE Robotics and Automation Society, pp. 1-6, 1993.

[17] Lee *et al.*, "A Miniaturized High-Voltage Solar Cell Array as an Electrostatic MEMS Power Supply", Journal of Microelectromechanical Systems, Vol. 4, No. 3, September 1995.

[18] Bates, J. B., Gruzalski, G. R., Luck, C. F., "Rechargeable Solid State Lithium Microbatteries", Proc. Micro Electro Mechanical Systems, IEEE Robotics and Automation Society, pp. 1-6, 1993.

[19] Brooks, K. P., Call, C. J., Drost, M. K., "Integrated Microchannel Combustor/Evaporator Development", Process Miniaturization: 2nd International Conference on Microreaction Technology, Topical Conference Reprints, 1998.

[20] Tonkovich *et al.*, "Microchannel Chemical Reactors for Fuel Processing", Process Miniaturization: 2nd International Conference on Microreaction Technology, Topical Conference Reprints, 1998.

[21] Hagendorf *et al.*, "A Pt/Al_2O_3 Coated Microstructured Reactor/Heat Exchanger for Controlled H_2/O_2-Reaction in the Explosion Regime", Process Miniaturization: 2nd International Conference on Microreaction Technology, Topical Conference Reprints, 1998.

[22] Groshenry, C., "Preliminary Study of a Micro-Gas Turbine Engine", S.M. Thesis, Massachusetts Institute of Technology, 1995.

[23] Miyajima, H., Mehregany, M., "High-Aspect Ratio Photolithography for MEMS Applications", Journal of Microelectromechanical Systems, Vol. 4., No. 4, pp. 220-229, December 1995.

[24] Robert Bosch Gmbh, Patents 4855017 and 4784720 (USA), and 4241045C1 (Germany).

[25] Klaassen *et al.*, "Silicon Fusion Bonding and Deep Reactive Ion Etching: A New Technology for Microstructures", The 8th International Conference on Solid-State Sensors and Actuators, and Eurosensors IX, Stockholm, 1995.

[26] Hsu, C. H., Schmidt, M. A., "Micromachined Structures Fabricated Using a Wafer Bonded Sealed Cavity Process", Technical Digest, IEEE Sensors Workshop, Hilton Head, SC, pp. 151-155, 1994.

[27] Ayón *et al.*, "Etching Characteristics and Profile Control in a Time Multiplexed Inductively Coupled Plasma Etcher", presented at the Solid-State Sensor and Actuator Workshop at Hilton Head, 1998.

[28] Kern, W., Puotinen, D. A., "Cleaning Solutions Based on Hydrogen Peroxide for Use in Silicon Semiconductor Technology", RCA Review, Vol. 31, pp. 187-206, 1970.

[29] Schmidt, M. A., "Silicon Wafer Bonding for Micromechanical Devices", presented at the Solid-State Sensor and Actuator Workshop at Hilton Head, 1994.

[30] Mehra, A., Waitz, I. A., "Development of a Hydrogen Combustor for a Microfabricated Gas Turbine Engine", presented at the Solid-State Sensor and Actuator Workshop at Hilton Head, 1998.

[31] Deal, B. E., Grove, A. S., "General Relationships for the Thermal Oxidation of Silicon", Journal of Applied Physics, Vol. 36, p. 3770, 1965.

[32] Spearing, S. M., Chen., K. S., "Micro-Gas Turbine Engine Materials and Structures", Presented at the 21st Annual Cocoa Beach Conference and Exposition on Composites, Advanced Ceramics, Materials and Structures, 1997.

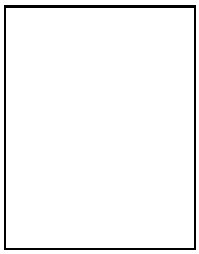

Amit Mehra received his B.S. degree in Engineering and Applied Science from the California Institute of Technology in June, 1995. He received his S.M. in Aeronautics and Astronautics from the Massachusetts Institute of Technology in June, 1997.
He is currently a doctoral student at the Gas Turbine Laboratory at MIT. His areas of interests include turbomachinery fluid dynamics, combustion and MEMS. He is member of the American Society of Mechanical Engineers, the American Institute of Aeronautics and Astronautics, Tau Beta Pi National Engineering Honor Society and the Sigma Xi National Research Society.

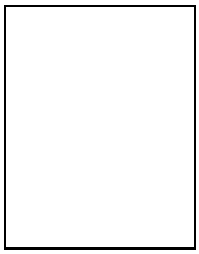

Arturo A. Ayón was born in Navojoa, Sonora, Mexico on July 17, 1958. He received his B.S. degree in Electronic Engineering from the Universidad de Guadalajara in Mexico in 1983, and his Ph.D. degree in Nuclear Science and Engineering from Cornell University in 1996.
In 1983, he joined the IBM computer manufacturing facility in Guadalajara, Mexico as a manufacturing engineer. In the same year, he moved to Rochester, MN to serve as engineering liaison between the IBM manufacturing plant in Mexico and the IBM development plant in the U.S. In 1985, he was appointed manufacturing and quality engineering manager and returned to Mexico to oversee the operation of the newly installed manufacturing lines for computer systems. In 1986, Dr. Ayón opened a marketing and distribution center for plastic commodities in Guadalajara, Mexico. He later sold

this operation to return to graduate school.

Dr. Ayón is currently a Research Scientist at the Massachusetts Institute of Technology, which he joined in 1996. He is involved in the development and microfabrication of turbomachinery and power generation devices. His interests include deep reactive ion etching, wafer bonding, low-k dielectrics and thin film characterization. He actively participates in the emerging field of power MEMS. Dr. Ayón in a member of the American Vacuum Society, The Electrochemical Society and the Electron Devices Society of the Institute of Electrical and Electronics Engineers.

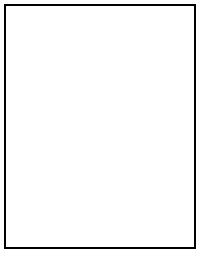

Ian A. Waitz is an Associate Professor of Aeronautics and Astronautics at the Massachusetts Institute of Technology, where he is Director of the MIT Aero-Environmental Research Laboratory and the Associate Director of the MIT Gas Turbine Laboratory. His principal fields of interest include propulsion, fluid-mechanical mixing, reacting flows, aeroacoustics, and in particular, aspects of the above which relate to environmental issues associated with aircraft design and propulsion. Professor Waitz currently directs a variety of experimental and computational research in these areas including studies of streamwise-vorticity-enhanced mixing, mixer-ejector design, jet noise reduction, mixing technology for low-emissions combustors, wake management strategies for fan noise reduction, pollutant chemistry in turbine nozzle flows, combustion processes for micro gas turbine engines, and vortical flows in compressor endwall flow fields.

Professor Waitz received a Ph.D. in Aeronautics from the California Institute of Technology in 1991, an M.S. in Aeronautics from George Washington University's Joint Institute for Advancement of Flight Sciences at NASA Langley Research Center in 1988, and a B.S. in Aerospace Engineering from Pennsylvania State University in 1986.

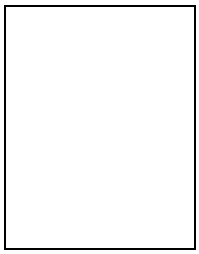

Martin A. Schmidt received the B.S. degree in electrical and computer engineering from Rensselaer Polytechnic Institute, Troy, NY, in 1981. He received the S.M. and Ph.D. degrees in electrical engineering and computer science (EECS) from the Massachusetts Institute of Technology (MIT), Cambridge, in 1983 and 1988, respectively.

His Ph.D. research was on microsensors for measurement of turbulent boundary layers. He joined the faculty of the EECS department of MIT in 1988, where he is currently a Professor of Electrical Engineering. He is also the Director of the Microsystems Technology Laboratories at MIT. His research interests are in microfabrication technologies for realization of micromechanical and biological reactors, micromachined turbine engines, and microactuators. He has served on the program committees for many of the major meetings in the MEMS field and currently serves on the International Steering Committee for Solid-State Sensors and Actuators.

Dr. Schmidt received the National Science Foundation Presidential Young Investigator Award and the Ruth and Joel Spira Teaching Award at MIT.

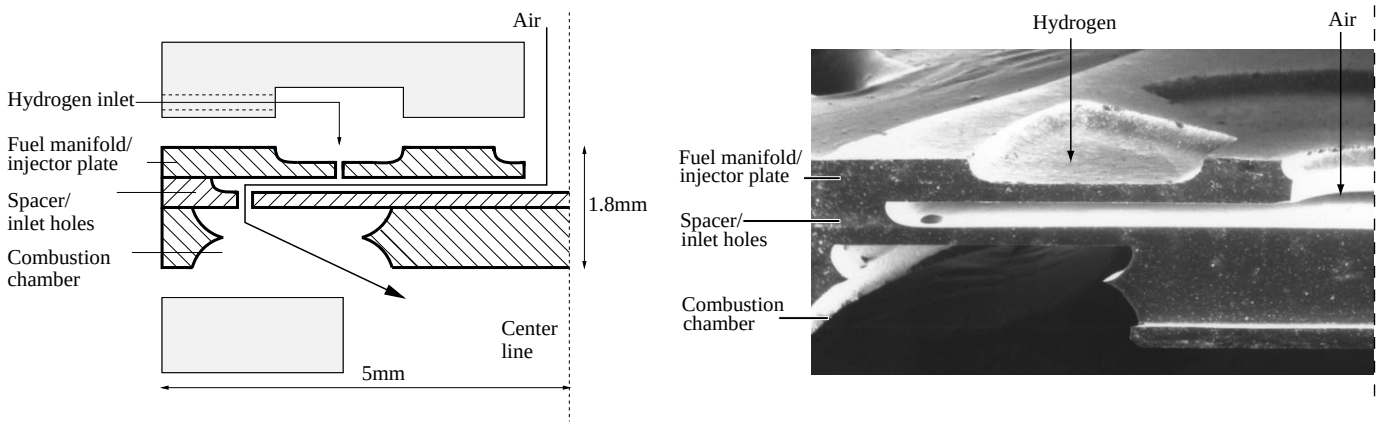

Fig. 1. Schematic and SEM cross-section of half of the axisymmetric combustor, showing the fuel manifold, injectors, and air flow path.

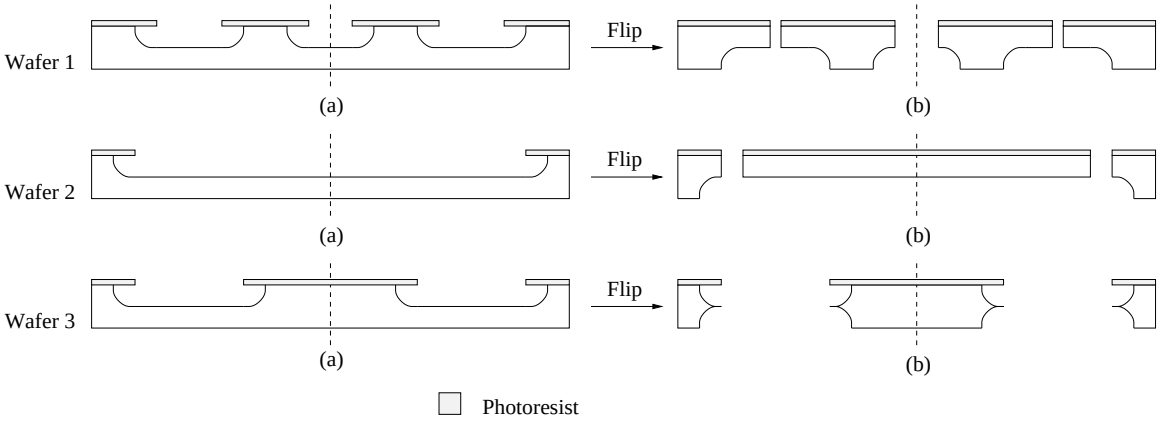

Fig. 2. Fabrication process for the microcombustor.

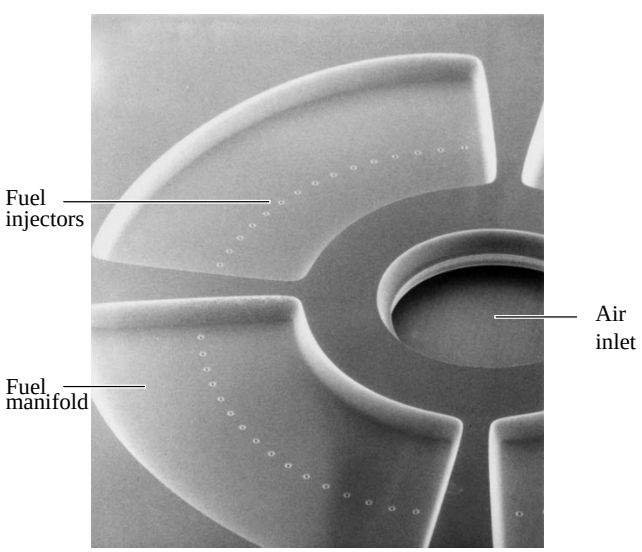

(a) SEM of the fuel manifold, showing a ring of 76, 30 μm injector holes.

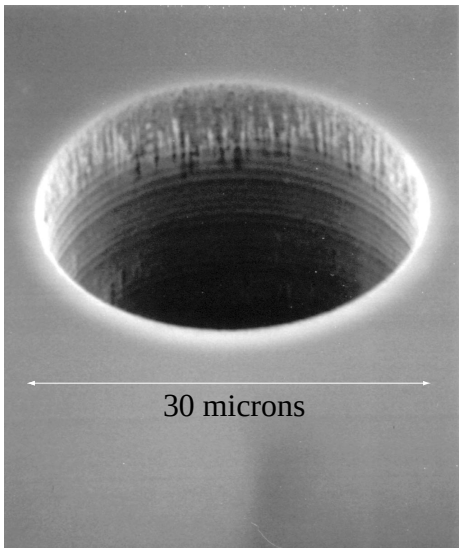

(b) Close-up view of a 200 μm deep, 30 μm diameter fuel injector hole.

Fig. 3. Fuel manifold / injector wafer (400 μm thick).

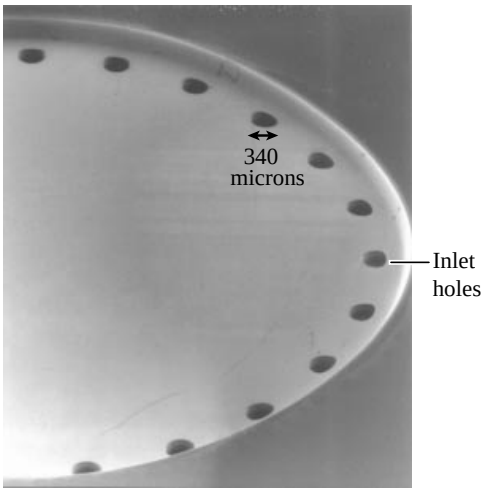

Fig. 4. Isotropically etched spacer plate, showing the 24, 340 μm combustor inlet ports at $r = 4.5$ mm.

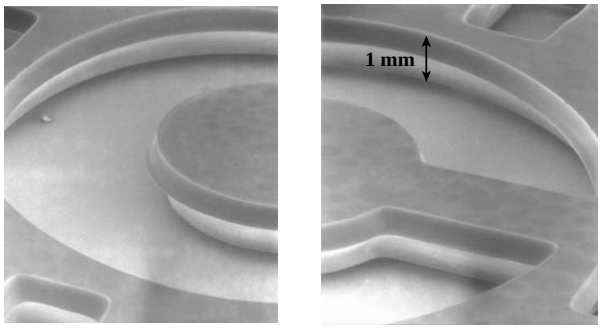

Fig. 5. Isotropically etched, 1 mm high annular combustion chamber, with an inner and outer diameter of 5 mm and 10 mm respectively.

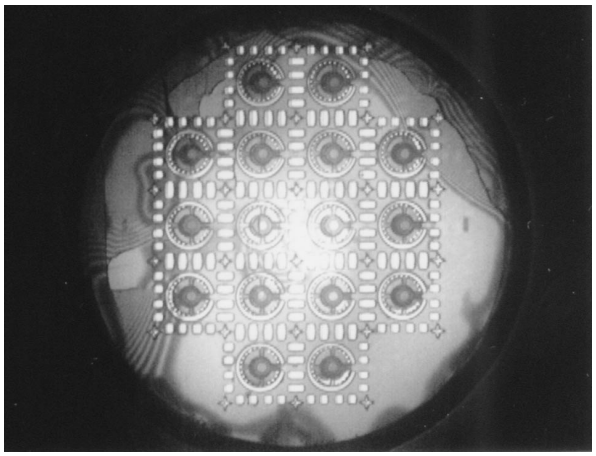

Fig. 6. Infra-red image of the three stack, double-bonded wafers, indicating a high quality bond over most of the wafer. The fringes on the edges indicate poor bond quality in these regions.

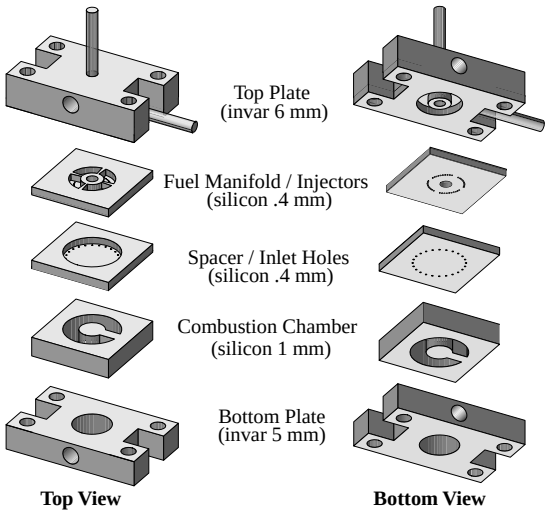

Fig. 7. A schematic of the microcombustor test rig (wafer thicknesses are exaggerated for illustrative effect).

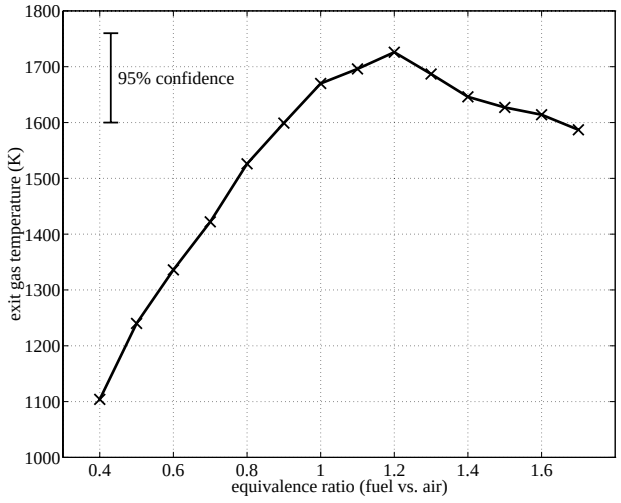

Fig. 8. Microcombustor test results, showing exit temperatures in excess of 1600K.

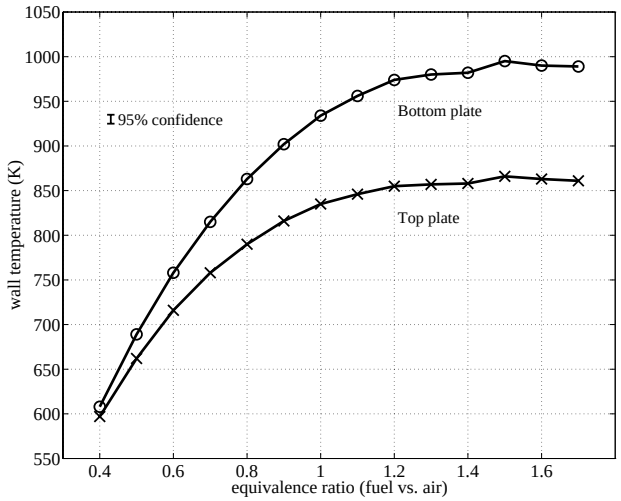

Fig. 9. Microcombustor test results, showing wall temperatures well below the melting point of silicon.

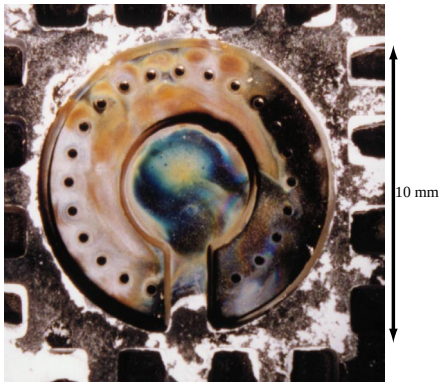

Fig. 10. Post-combustion appearance of the rig after 15 hours of testing at T_{exit} ~1600K. While the oxidation patterns are apparent, the structure shows no visible damage (the white regions represent ceramic adhesive used for sealing).

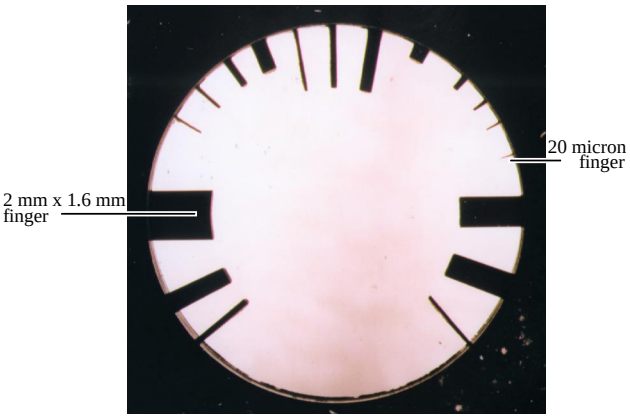

Fig. 11. Photograph of the silicon combustor plate with "finger-like" structures (sizes range between 20 μm $\times$ 500 μm $\times$ 450 μm and 1600 μm $\times$ 2000 μm $\times$ 450 μm).

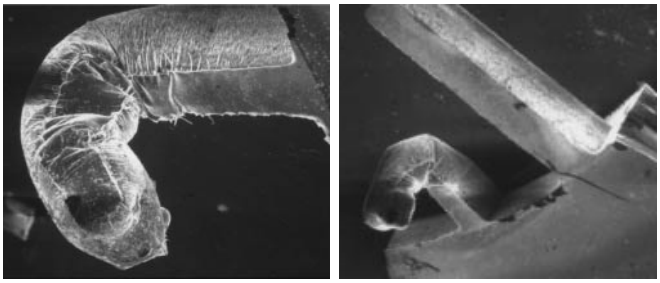

Fig. 12. SEM of a 200 μm $\times$ 450 μm $\times$ 2000 μm structure after combustion, showing creep limited performance of silicon.

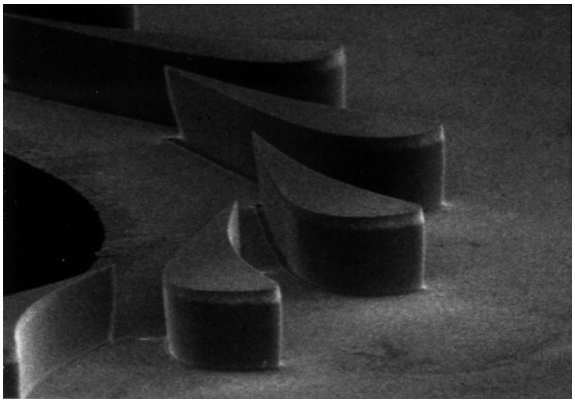

Fig. 13. An SEM of the turbine static vane pack that was attached to the combustor exhaust plate to study the structural behavior of the blades when exposed to combustion exhaust gases.

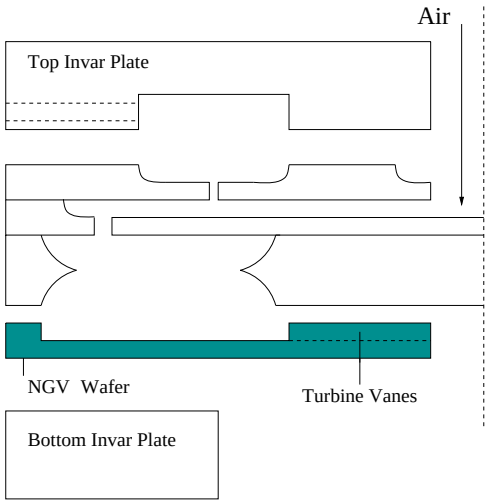

Fig. 14. A schematic illustration of the placement of the turbine vanes in the microcombustor test rig.

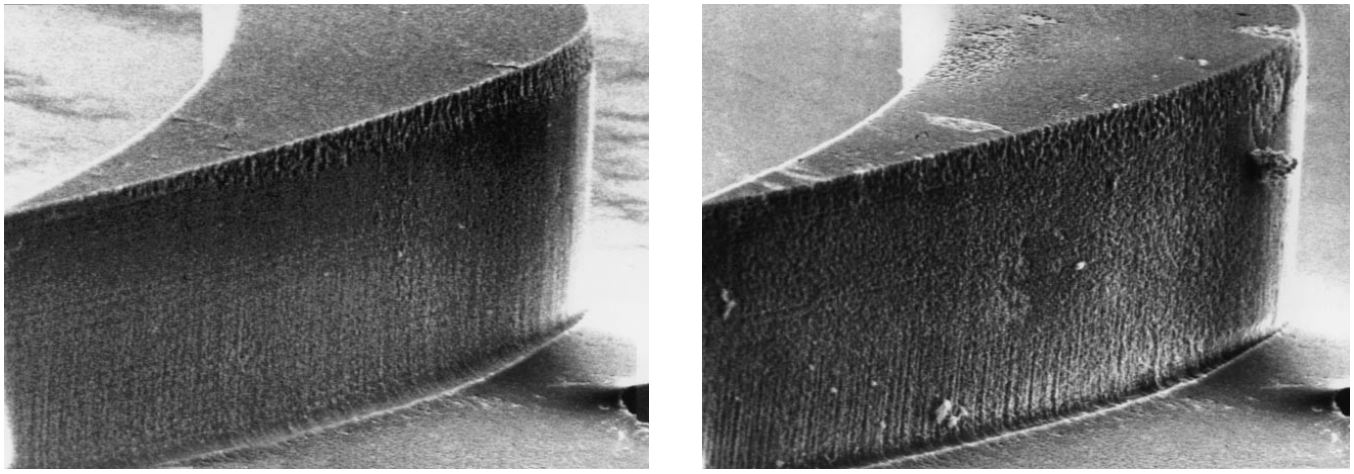

Fig. 15. Before and after pictures of the vanes following a 5 hour exposure to combustion exhaust gases at 1800K, Mach number ~ 1. Although the blades exhibit minor erosion and "pitting", they maintain their structural integrity.